Biochemical and Biophysical Research Communications 458 (2015) 644–649

Contents lists available at ScienceDirect

Biochemical and Biophysical Research Communications

journal homepage: www.elsevier.com/locate/ybbrc

Structure analysis of *Bacillus cereus* MepR-like transcription regulator, BC0657, in complex with pseudo-ligand molecules☆

Meong Il Kim, Min Uk Cho, Minsun Hong*

Division of Biological Science and Technology, Yonsei University, Wonju 220-710, Republic of Korea

ARTICLE INFO

Article history:
Received 16 January 2015
Available online 13 February 2015

Keywords:
Bacillus cereus
BC0657
MepR
MarR
Crystal structure

ABSTRACT

The MarR family of transcriptional regulatory proteins in bacteria and archaea respond to environmental changes and regulate transcriptional processes by ligand binding or cysteine oxidation. MepR belongs to the MarR family, and its mutations are associated with the development of multidrug resistances, causing a growing health problem. Therefore, it has been of great interest to locate the ligand binding site of MepR and reveal the ligand-mediated transcriptional regulation mechanism. Here, we report on the crystal structure of *Bacillus cereus* MepR-like transcription factor, BC0657, at 2.16 Å resolution. Interestingly, BC0657 was complexed with fortuitous pseudo-ligands, which were assessed to be lipid molecules containing a long fatty acid, rather than phenolic compounds previously observed in other MarR proteins. The BC0657-ligand interaction provides the first molecular view of how MepR recognizes ligands to respond to toxic chemicals. Moreover, our comparative structure analyses of ligand binding sites on BC0657 and its homologs suggest that transcriptional repression by MepR would be relieved by ligand-induced changes in dimerization organization.

1. Introduction

Bacteria have developed a variety of molecular protection systems against harmful environmental chemicals and stresses. Multiple antibiotic resistance regulator (MarR) family proteins are transcriptional regulators that modulate the expression of genes involved in oxidative stress responses as well as degradation or export of toxic chemicals, such as phenolic compounds, antibiotics, and detergents [1–6]. The MarR protein was first reported in *Escherichia coli* and is now one of the largest transcription regulator families, including over 15,800 members (http://www.ebi.ac.uk/interpro/entry/IPR000835/proteins-matched). *E. coli* MarR negatively regulates gene expression of the *marRAB* operon by binding to the operator DNA upstream of the transcription start site and inhibiting RNA polymerase-mediated transcription initiation. MarR binding to its ligand, such as sodium salicylate, attenuates the MarR–operator interaction, allowing RNA polymerase to initiate transcription of the resistance gene [7,8].

Structural and biochemical studies have been performed on numerous MarR family members to date. Despite the large variation in primary sequences, MarR proteins adopt the triangular shape of a homodimer with the similar structural fold of the winged helix-turn-helix (wHTH) domain and the homodimerization domain [6,9]. It is well documented that the two wHTH domains of the triangular homodimer recognize palindromic sequences of double-stranded DNA in a symmetrical manner [10–15]. However, for the transcriptional regulation mechanism, each MarR protein appears to have developed a unique ligand recognition mode and, consequently, undergoes different conformational changes upon ligand binding. Several complex structures with ligand/drug molecules have independently allowed for the identification of up to eight discrete, ligand-binding sites for one MarR protomer, indicating multiple regulatory mechanisms in the MarR family [9,16–18].

MepR from *Staphylococcus aureus* belongs to the MarR family and is a multidrug-binding transcription regulator for expression of *mepA* and *mepR* [19,20]. MepA is a multidrug efflux pump that confers resistance to a wide range of toxic compounds, including biocides, fluoroquinolones, glycylcycline, tigecycline, and dyes.

☆ **Data deposition**: The atomic coordinates and structural factors for BC0657 (PDB ID 4XRF) have been deposited in the Protein Data Bank, www.pdb.org.

* Corresponding author. 1 Yonseidae-gil, Mirae Building #303, Wonju 200-710, Republic of Korea. Fax: +82 33 760 2183.
E-mail address: minsunhong@yonsei.ac.kr (M. Hong).

http://dx.doi.org/10.1016/j.bbrc.2015.02.019
0006-291X/

Mutations of the *mepR* gene [replacements of glutamine for proline residue at 18 (Q18P), of phenylalanine for leucine at 27 (F27L), and of alanine for valine at 103 (A103V)] have been associated with multidrug-resistance of clinical *S. aureus* isolates [21]. A recent structural study revealed that the MepR mutations were located in the dimerization interface and caused severe distortions in quaternary conformations of the MepR dimer [15]. However, due to the absence of the MepR-ligand complex structure, it is currently unclear how the MepR transcription factor recognizes ligand molecules to function as a transcriptional regulator.

Here we present the crystal structure of *Bacillus cereus* MepR-like transcription regulator, BC0657, at 2.16 Å resolution. BC0657 is homodimeric and contains the canonical wHTH domain, as is found in other MarR transcriptional regulators. Interestingly, extra electron density was observed inside a hydrophobic cavity in the dimerization interface and was assessed as fortuitous lipid-like pseudo-ligands. Furthermore, our comparative structural analyses suggest an allosteric mechanism for ligand-mediated disruption of the MepR–operator interaction.

2. Materials and methods

2.1. Preparation of the recombinant BC0657 protein

BC0657 expression plasmid was prepared and recombinant BC0657 protein was expressed and purified as described elsewhere (paper in preparation). Briefly, the BC0657 gene (residues 1–152) was amplified by PCR from the genome DNA of *B. cereus* and inserted into a modified pET49b vector (pET49bm) that contains the N-terminal His_6 tag and thrombin cleavage site. The resulting ligation product was transformed into *E. coli* DH5α cells and nucleotide sequences were confirmed by DNA sequencing.

Recombinant BC0657 protein was overexpressed in the *E. coli* strain, BL21 (DE3) in the presence of 1 mM isopropyl β-D-1-thio-galactopyranoside at 18 °C for ~16 h. Cells were harvested and lysed by sonication. The lysate was cleared by centrifugation (~25,000 × g) and the supernatant was incubated with Ni-NTA resin (Qiagen). The soluble BC0657 protein was eluted using PBS containing 250 mM imidazole, and dialyzed against 20 mM Hepes, pH 7.4/150 mM NaCl/5 mM β-mercaptoethanol (βME). The N-terminal His_6 tag was removed by thrombin and was further purified by gel filtration chromatography using a Superdex 200 16/600 column (GE Healthcare) in 20 mM Hepes, pH 7.4/150 mM NaCl/5 mM βME. Fractions for BC0657 were pooled and concentrated to ~34 mg/ml for crystallization.

2.2. BC0657 crystallization and X-ray diffraction data collection

The BC0657 protein was crystallized by the sitting drop vapor diffusion method at 18 °C. BC0657 crystals were obtained in 0.1 M phosphate citrate, pH 4.0/1.8 M ammonium sulfate. For X-ray diffraction data collection, BC0657 crystals were cryoprotected in a solution of 0.1 M phosphate citrate, pH 4.0/2.4 M ammonium sulfate/30% glycerol. A single crystal was flash-frozen under the cryostream at −173 °C. X-ray diffraction was performed at beamline 7A of the Pohang Accelerator Laboratory (PAL). Diffraction data were indexed, integrated, and scaled using the HKL2000 package [22]. X-ray diffraction statistics are shown in Table S1.

2.3. Structure determination of BC0657

The BC0657 structure was determined by molecular replacement with the *PHASER* program [23] using structure coordinates (PDB ID IS3J) of a MarR protein, YusO, as a search model. The BC0657 structure was iteratively built and refined using the *COOT* and *REFMAC5* programs, respectively [24,25]. The final model includes residues 5–146, 69 waters, and putative lipid-like pseudo-ligand molecules. The final model has excellent stereochemistry, with no Ramachandran outliers [28]. Structure refinement statistics are shown in Table S1.

3. Results

3.1. The overall crystal structure of BC0657

The BC0657 structure was solved by molecular replacement and refined to 2.16 Å resolution (Table S1). The asymmetric unit (ASU) contains one chain of BC0657 (Fig. 1A). The BC0657 structure contains 142 residues (residues 5–146) from the entire molecule (residues 1–152). The overall fold of BC0657 is similar to those of other MarR family members consisting of six helices and three β strands with a topology of H1 (residues 8–33) – H2 (residues 37–49) – β1 (residues 51–53) – H3 (residues 54–61) – H4 (residues 65–77) – β2 (81–85) – β3 (93–97) – $H5^a$ (99–111) – $H5^b$ (114–121) – H6 (126–143) (Fig. 1A and B). The non-helical nature of the BC0657 at residue 113 divides helix 5 into two separate helices, $H5^a$ and $H5^b$. Single-turn 3_{10} helices are also observed in residues 59–61, 65–57, 76–78, 108–110, and 125–127. As for other MarR protein structures, the BC0657 monomer is divided into two functional domains, the dimerization domain and the wHTH domain. The dimerization domain involves the N- and C-terminal helices (H1, H2, H5, and H6) and mediates BC0657 homodimerization. The wHTH domain consists of β1, H3, H4, β2, and β3, and is a putative DNA binding domain.

DALI analyses indicate that the BC0657 structure is closely related to other MarR family proteins, including *S. aureus* MepR Q18P mutant (PDB ID 4LD5; RMSD value of 2.9 Å for 137 residues; 21% sequence identity), *Bacillus subtilis* YusO (PDB ID 1S3J; RMSD value of 3.9 for 129 residues; 32% sequence identity), *B. subtilis* OhrR (BsOhrR, PDB ID 1Z9C; RMSD value of 4.0 for 137 residues; 18% sequence identity), and *Streptomyces coelicolor* PcaV (PDB ID 4FHT; RMSD value of 3.3 for 137 residues; 16% sequence identity) (Fig. 1B). The wHTH domains of MarR homologs superpose well on that of BC0657, whereas dimerization domains showed severe structural deviations (Fig. 1C).

3.2. The dimerization interface of the BC0657 protein

MarR family proteins function as homodimers. Consistently, BC0657 forms a crystallographic dimer (Fig. 1D). The dimerization interface of BC0657 is mainly constituted by helices H1, H2, H5, and H6 of the dimerization domain and supplemented by additional residues including residue 60 of helix H3 and residues 61-62 of an H3–H4 linker. Dimerization of BC0657 buries an accessible surface area of 2180 $Å^2$ per subunit mostly by hydrophobic interactions, as is found in other MarR members [9,10,16].

In the BC0657 structure, it is noteworthy that the N-terminal helix H1 is simultaneously engaged in various interactions, including intra-subunit H1–H5 interactions, homodimeric assembly, and BC0657-ligand recognition (Fig. 2). A C-terminal part (residues 21–33) of H1 makes extensive intra-subunit interactions with H5 (Arg104, Glu107, Ala108, Ala111, Arg112, Asn113, His115, Ile116, and Tyr119), suggesting that the C-terminal H1 is essential in the formation of the globular monomeric fold (Fig. 2C). In contrast to the C-terminal H1, the N-terminal region of H1 (residues 8–20) protrudes out of the monomer without significant contribution to intra-subunit interactions (Fig. 1A). Instead, the N-terminal H1 is plugged inside a bundle of helices of the other subunit, including H2′, H3′, H5′, and H6′ (the prime symbol denotes a 2-fold symmetry-related molecule) and plays a primary role in

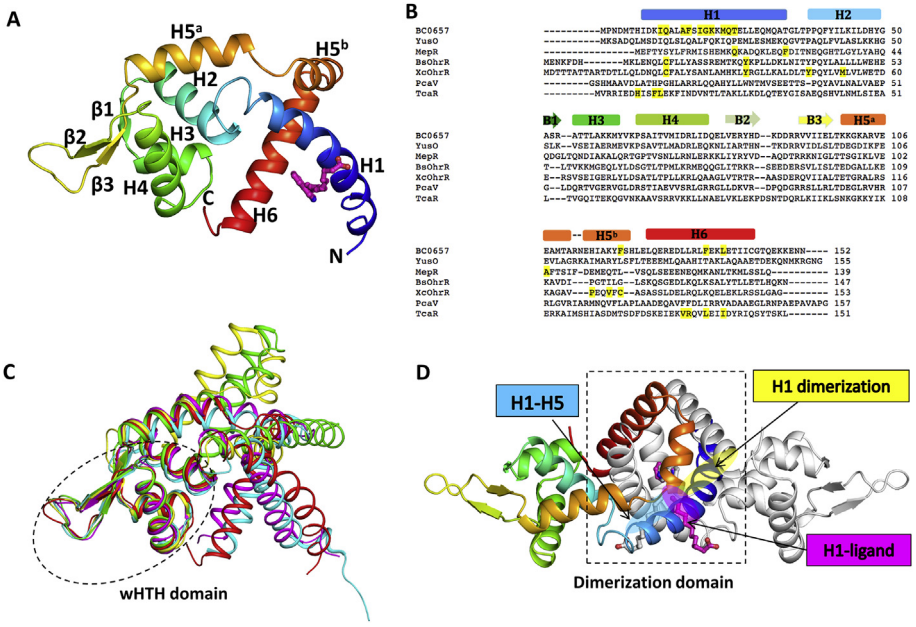

Fig. 1. Overall structure of BC0657. (A) A ribbon diagram of one BC0657 subunit complexed with pseudo-ligand molecules (ball-and-stick models). The structure is rainbow-colored from blue at the N-terminus to red at the C-terminus. The secondary structures are labeled and the N- and C-terminal ends of BC0657 are indicated as N and C, respectively. (B) Primary sequence alignment of BC0657 and its structural homologs in the MarR family (YusO, MepR, BsOhrR, XcOhrR, PcaV, TcaR). The multiple sequence alignment was performed using ClustalW. The secondary structural elements of BC0657 are indicated by rods (α- and 3_{10}-helices) and arrows (β-strands) in rainbow colors above the primary sequence of BC0657. Ligand binding or sensing residues are shaded in yellow, except for MepR, in which multidrug resistant mutation residues are highlighted in yellow. (C) Structural comparison of MarR family proteins [BC0657 (red), MepR (yellow), YusO (green), PcaV (magenta), and BsOhrR (cyan)]. wHTH domains are circled in dashes. D. Ribbon diagram of the BC0657 dimer in complex with pseudo-ligands (ball-and-stick models). One subunit is colored in rainbow and its dyadic mate is colored in gray. The dimerization domain is highlighted in a dotted box. Interfaces mediated by H1 residues (H1–H5 contact, H1 dimerization, and H1-ligand recognition) are labeled and colored accordingly. (For interpretation of the references to color in this figure legend, the reader is referred to the web version of this article.)

dimerization (Figs. 1D and 2). The center of the H1 helix is involved in pseudo-ligand binding (see below). As a result, the H1 helix buries a total surface area of 1234 Å^2 (the H1–H5 contacts, 276 Å^2; H1-ligand contacts, 203 Å^2; H1 dimerization contacts, 755 Å^2) via mostly hydrophobic and some hydrophilic interactions. Four and five hydrogen bonds are observed in the H1–H5 contact (Glu25-Tyr119, Glu25-Asn113, Thr33-Arg104, and Gly34-Arg104) and the H1-dimerization interface (Thr6-Arg128′, His7-Glu129′, Asp9-Lys44′, Lys10-Try41′, and Gln23-Gln23′), respectively. In addition, three salt bridges are formed between Asp9 and Arg112′, and between Lys10 and Glu136.

3.3. *Fortuitous lipid-like pseudo-ligands in the hydrophobic cavity of BC0657*

A striking feature of the BC0657 crystal structure is that tadpole-shaped electron density was additionally observed in the Fo–Fc map, even after the protein part was completely built in the structure model (Fig. 3A). The extra density was found in a cavity formed in the dimerization interface (Fig. 3B). The head portion of the tadpole-shaped electron density (density site-A) penetrates deeply into the cavity, whereas the tail (density site-B) is partially buried and stretched along the BC0657 surface. The electron density

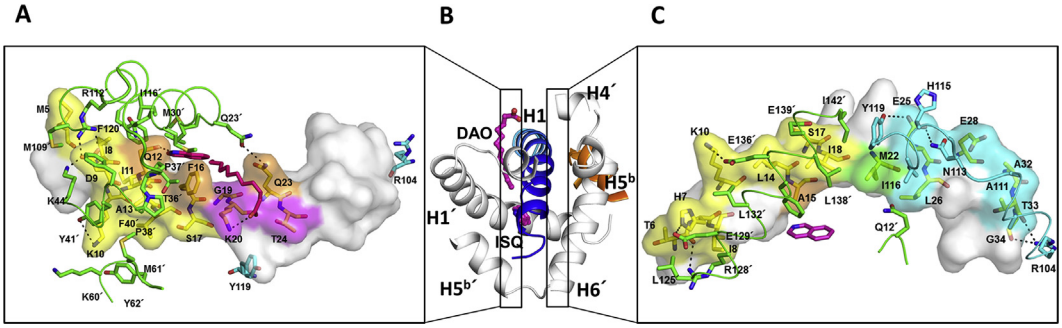

Fig. 2. Simultaneous engagement of BC0567 helix H1 in inter-subunit, intra-subunit, and pseudo-ligand interactions. (A) and (C) are open-book views of BC0657 dimerization interactions in (B). (B) H1 and H5^b of one subunit are colored in a manner identical to that of Fig. 1A and helices from the second subunits are colored in gray. (A and C) Interfaces for dimerization, pseudo-ligand binding, and intra-subunit H1–H5 interaction are colored in yellow, magenta, and cyan, respectively, on the H1 surface. Interface residues involved in both dimerization and lipid binding (Gln12, Ala5, Phe16, and Gln23) and in both lipid binding and H1–H5 interaction (M22) are highlighted in orange or green surfaces, respectively. BC0657 interface residues are also depicted by sticks (carbon; yellow, oxygen; red, nitrogen; blue). Residues from dimerization partners, lipid molecules, and H5 residues are shown in green, magenta, and cyan ball-and-stick models, respectively, with oxygen atoms in red and nitrogen atoms in blue. Dashed lines represent hydrogen bonds and salt bridges. (For interpretation of the references to color in this figure legend, the reader is referred to the web version of this article.)

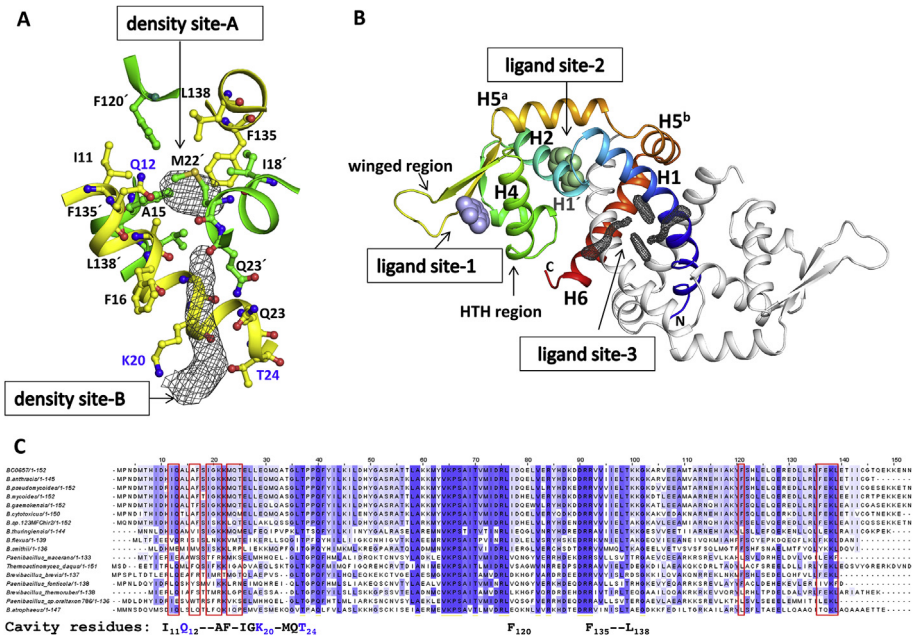

Fig. 3. Pseudo-ligand binding sites in the BC0657 dimerization interface. (A) Two electron density sites, A and B, (2.0 σ level in the Fo–Fc composite omit map) inside the hydrophobic cavity in the dimerization interface. The two subunits of BC0657 are shown in different colors, yellow and green. BC0657 residues that surround the density sites are shown in ball-and-stick models. (B) Ligand sites of MarR family members. Representative ligand sites are assigned by ligand site-1-3 (ligand site-1, light blue, PDB ID 1JGS and 4EM0; ligand site-2, light green, PDB ID 4FHT, 3BPX and 3GF2; ligand site-3, PDB ID 3KP6 and 2PFB). Ligand site-1 of MarR is formed between recognition helix H4 and the winged regions. Ligand site-2 is generated between helix H4 of the wHTH domain and helix H1′ of the dimerization domain in ST1710. Pseudo-ligands of BC0657 in gray wires are co-localized with ligand site-3 of TcaR and XcOhrR. (C) Sequence conservation of cavity-forming residues in BC0657 homologs. Amino acid sequences were aligned by ClustalW and colored by JalView. Pseudo-ligand binding residues are boxed in red and their consensus sequences are shown below the alignment with polar residues colored in blue. (For interpretation of the references to color in this figure legend, the reader is referred to the web version of this article.)

for a linker between density site-A and site-B was very weak, presumably due to the high flexibility in the middle of one molecule or the presence of two separate molecules.

The internal volume of the cavity surrounding density sites-A and -B, is estimated to be ~360 Å^3 [26]. The cavity was formed by H1, H2, β1, H1′, and H5′ residues (Ile11, Gln12, Ala15, Phe16, Gly19, Lys20, Gln23, Thr24, Phe135, Leu138, Ile18′, Gly19′, Met22′, Gln23′, Phe120′, and Phe135′). The cavity-forming residues are highly conserved in BC0657 homologs with at least 61% sequence identity (Fig. 3C). The internal surface of the cavity is highly hydrophobic except for the oxygen atom (OE1) of Gln12 at density site-A, and for the positively charged nitrogen atom (NZ) of Lys20 at the cavity entrance in density site-B. Interestingly, negatively and positively charged side atoms at Gln12 and Lys20 are absolutely conserved in BC0657 homologs by chemically homologous changes to glutamate (Q/E), and arginine or glutamine (K/R/Q), respectively (Fig. 3C and Fig. S2), suggesting that the two polar residues, Gln12 and Lys20, play a critical role in ligand specificity in the hydrophobic environment. These observations demonstrate that hydrophobic cavity sites with partial charges at dimerization domains are common features in BC0657 and its homologs. Moreover, the pseudo-ligand would be a charged lipid-like molecule, such as a lipid molecule containing an extended hydrophobic acyl chain.

The shape of the electron density and the chemical nature of its environment allowed us to separately build isoquinoline (ISQ) and lauric acid (dodecanoic acid; DAO) as pseudo-ligand molecules into elliptical head density (density site-A) and elongated tail density (density site-B), respectively, although we cannot rule out possibilities of other abundant cellular lipids or drugs (Fig. 3A and Fig. S1A). ISQ and DAO fit well into density sites-A and -B, respectively, and were in good agreement with refinement statistics. The N2 nitrogen atom of ISQ and the carboxylic oxygen atom of DAO preferentially interact with the polar side chain of Gln12 (distance between Gln12 OE1 and ISQ N2, 2.9 Å) in density site-A and the positive charge of Lys20 (distance between Lys20 NZ and DAO O1, 3.2 Å) in density site-B, respectively (Fig. S1).

3.4. Comparisons of ligand binding sites of BC0657 with other MarR proteins

Most MarR proteins sense a variety of lipophilic compounds, and OhrR and SarZ respond to oxidative stresses. Structural studies on oxidized *Xanthomonas campestris* OhrR (XcOhrR) [27] and MarR-lipophilic drug complexes, including MarR-salicylate [9,17], ST1710-salicylate [14], PcaV-protocatechuate (PcaV) [16], MarR-kanamycin, and TcaR-salicylate (TcaR) [18] have identified eight discrete ligand binding sites, three of which have been confirmed as physiologically relevant ligand binding and functional regulatory sites (ligand sites-1, -2 and -3) (Fig. 3B). MarR ligand site-1 and ST1710 ligand site-2 involve residues from the DNA binding region of the wHTH domain and thus, ligand association directly inhibits DNA binding. In contrast, ligand site-3 in the oxidized XcOhrR and the TcaR-salicylate complex was constituted by residues only from dimerization helices H1 and H5, and ligand associations induce conformational changes of quaternary structures to disable the wHTH domain in DNA binding (Fig. 3B). The BC0657 cavity that encloses the pseudo-ligand molecules is positioned in the dimerization domains and overlaps with ligand site-3. Since the pseudo-ligand binding site of BC0657 does not involve any residues from the wHTH domain, BC0657 ligand would not directly compete with DNA for BC0657. Instead, ligand binding to BC0657 would induce structural rearrangements to dissociate wHTH domains from operator DNA through an allosteric regulatory mechanism as for XcOhrR and TcaR.

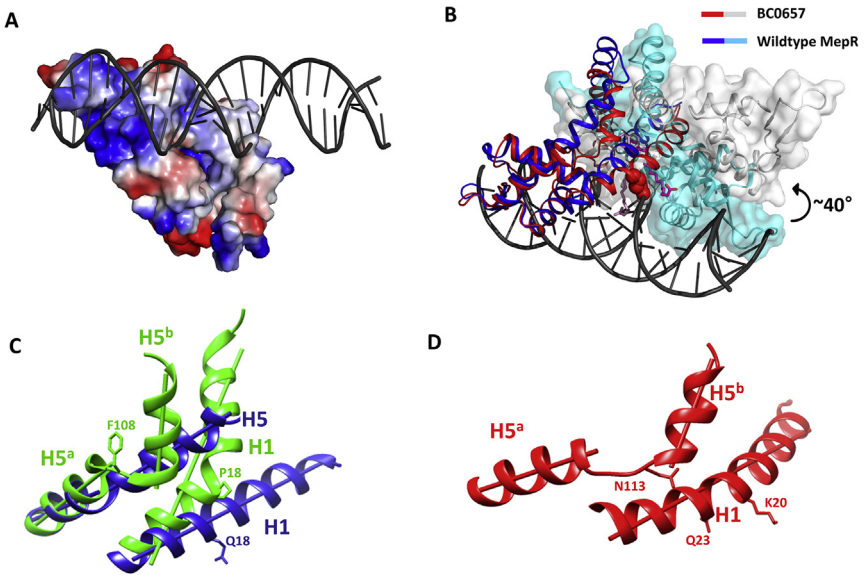

Fig. 4. DNA binding of BC0657. (A) A model of BC0657 in complex with dsDNA. The model was generated by overlaying the wHTH motif of BC0657 on that of the MepR–DNA structure (PDB ID 4LLN). BC0657 and dsDNA are shown in electrostatic surface potentials (positive charge, blue; negative charge, red) and in the dark gray cartoon, respectively. (B) Structural overlay of the MepR–DNA complex (PDB ID 4LLN; blue and cyan) and the BC0657–DNA model (red and gray). dsDNA is represented by a dark gray cartoon and proteins are shown in ribbons and transparent surface representations. In the BC0657–DNA model, Gln23 (red spheres) and pseudo-ligands (magenta and light pink sticks) sterically crash collide with DNA molecules. (C and D) Distorted dimerization helices H1 and H5 of MepR Q18P mutant and pseudo-ligand-bound BC0657 compared to wild-type MepR bound to DNA. Wild-type MepR, MepR Q18P, and BC0657 are shown in ribbons colored in blue, green, and red, respectively. Helical axes were calculated by the Chimera program and are shown by sticks inside helices. Some residues of MepR mutants positioned at 18 and 108 and of BC0657 at 20, 23, and 113 are shown by sticks for clarity. (For interpretation of the references to color in this figure legend, the reader is referred to the web version of this article.)

3.5. Implications of the BC0657 structure in the MerR transcription regulation mechanism

Structure surface analysis and DNA binding modeling suggest that the BC0657 monomer is able to interact with operator DNA. Based on electrostatic potential analysis, BC0657 exhibits highly positive patches in the wHTH domain, as is seen in other MarR proteins. In a BC0657 monomer–DNA complex model, positively charged Arg53, Lys59, and Lys64 from the helix-turn-helix motif and His85, Arg83, Arg90, and Arg91 from the winged region of the wHTH domain are positioned into major and minor grooves, respectively, of B-form dsDNA, without noticeable steric crashes, and make attractive ionic interactions with negatively charged phosphate groups of dsDNA (Fig. 4A).

In contrast to monomer, the other subunit of the dimeric BC0657 structure does not optimally interact with dsDNA. When one subunit of dimeric BC0657 is superposed on the MepR–DNA complex structure, the wHTH domain of the second BC0657 subunit is rotated by ~40° away from the DNA and does not make any interactions with DNA (Fig. 4B). Interestingly, the DNA binding-incompatible conformation of the BC0657 dimer was recapitulated in the structure of the MepR Q18P mutant that is incapable of DNA binding. Dimerization helices are distorted via bent H1 and broken H5 into $H5^a$ and $H5^b$ in both BC0657 and MepR Q18P, and as a result, the second subunit is not able to make optimal contacts with dsDNA. Collectively, the BC0657 structure that we have determined represents a DNA binding-incompatible conformation of MepR-like transcription factor shaped by the presence of a pseudo-ligand. Finally, we propose, as an allosteric derepression mechanism, that pseudo-ligand binding can distort the dimerization interface of BC0657 and allow BC0657 to be released from operator DNA.

Conflict of interest

The authors declare that there are no conflicts of interest.

Acknowledgments

X-ray diffraction datasets were collected at beamline 7A of the Pohang Accelerator Laboratory (Korea). This study was supported by the Basic Science Research Program through the National Research Foundation of Korea (NRF) funded by the Ministry of Science, ICT and Future Planning (2013R1A1A1008707 to MH), and by a 2013 Research Grant from Yonsei University (2013625023 to MH).

Appendix A. Supplementary data

Supplementary data related to this article can be found at http://dx.doi.org/10.1016/j.bbrc.2015.02.019.

Transparency document

Transparency document associated with this article can be found in the online at http://dx.doi.org/10.1016/j.bbrc.2015.02.019.

References

[1] S.P. Cohen, H. Hachler, S.B. Levy, Genetic and functional analysis of the multiple antibiotic resistance (mar) locus in *Escherichia coli*, J. Bacteriol. 175 (1993) 1484–1492.
[2] R.R. Ariza, S.P. Cohen, N. Bachhawat, S.B. Levy, B. Demple, Repressor mutations in the marRAB operon that activate oxidative stress genes and multiple antibiotic resistance in *Escherichia coli*, J. Bacteriol. 176 (1994) 143–148.
[3] R.G. Martin, J.L. Rosner, Binding of purified multiple antibiotic-resistance repressor protein (MarR) to mar operator sequences, Proc. Natl. Acad. Sci. U.S.A. 92 (1995) 5456–5460.
[4] M.C. Sulavik, L.F. Gambino, P.F. Miller, The MarR repressor of the multiple antibiotic resistance (mar) operon in *Escherichia coli*: prototypic member of a family of bacterial regulatory proteins involved in sensing phenolic compounds, Mol. Med. 1 (1995) 436–446.
[5] M.N. Alekshun, S.B. Levy, Alteration of the repressor activity of MarR, the negative regulator of the *Escherichia coli* marRAB locus, by multiple chemicals in vitro, J. Bacteriol. 181 (1999) 4669–4672.

[6] I.C. Perera, A. Grove, Molecular mechanisms of ligand-mediated attenuation of DNA binding by MarR family transcriptional regulators, J. Mol. Cell Biol. 2 (2010) 243–254.
[7] M.N. Alekshun, S.B. Levy, The mar regulon: multiple resistance to antibiotics and other toxic chemicals, Trends Microbiol. 7 (1999) 410–413.
[8] S.P. Wilkinson, A. Grove, Ligand-responsive transcriptional regulation by members of the MarR family of winged helix proteins, Curr. Issues Mol. Biol. 8 (2006) 51–62.
[9] M.N. Alekshun, S.B. Levy, T.R. Mealy, B.A. Seaton, J.F. Head, The crystal structure of MarR, a regulator of multiple antibiotic resistance, at 2.3 A resolution, Nat. Struct. Biol. 8 (2001) 710–714.
[10] M. Hong, M. Fuangthong, J.D. Helmann, R.G. Brennan, Structure of an OhrR–ohrA operator complex reveals the DNA binding mechanism of the MarR family, Mol. Cell 20 (2005) 131–141.
[11] K.T. Dolan, E.M. Duguid, C. He, Crystal structures of SlyA protein, a master virulence regulator of Salmonella, in free and DNA-bound states, J. Biol. Chem. 286 (2011) 22178–22185.
[12] P. Brugarolas, F. Movahedzadeh, Y. Wang, N. Zhang, I.L. Bartek, Y.N. Gao, M.I. Voskuil, S.G. Franzblau, C. He, The oxidation-sensing regulator (MosR) is a new redox-dependent transcription factor in *Mycobacterium tuberculosis*, J. Biol. Chem. 287 (2012) 37703–37712.
[13] N. Quade, C. Mendonca, K. Herbst, A.K. Heroven, C. Ritter, D.W. Heinz, P. Dersch, Structural basis for intrinsic thermosensing by the master virulence regulator RovA of Yersinia, J. Biol. Chem. 287 (2012) 35796–35803.
[14] T. Kumarevel, T. Tanaka, T. Umehara, S. Yokoyama, ST1710–DNA complex crystal structure reveals the DNA binding mechanism of the MarR family of regulators, Nucleic Acids Res. 37 (2009) 4723–4735.
[15] I. Birukou, S.M. Seo, B.D. Schindler, G.W. Kaatz, R.G. Brennan, Structural mechanism of transcription regulation of the *Staphylococcus aureus* multidrug efflux operon mepRA by the MarR family repressor MepR, Nucleic Acids Res. 42 (2014) 2774–2788.
[16] J.R. Davis, B.L. Brown, R. Page, J.K. Sello, Study of PcaV from *Streptomyces coelicolor* yields new insights into ligand-responsive MarR family transcription factors, Nucleic Acids Res. 41 (2013) 3888–3900.
[17] V. Saridakis, D. Shahinas, X. Xu, D. Christendat, Structural insight on the mechanism of regulation of the MarR family of proteins: high-resolution crystal structure of a transcriptional repressor from *Methanobacterium thermoautotrophicum*, J. Mol. Biol. 377 (2008) 655–667.
[18] Y.M. Chang, W.Y. Jeng, T.P. Ko, Y.J. Yeh, C.K. Chen, A.H. Wang, Structural study of TcaR and its complexes with multiple antibiotics from *Staphylococcus epidermidis*, Proc. Natl. Acad. Sci. U.S.A. 107 (2010) 8617–8622.
[19] G.W. Kaatz, C.E. DeMarco, S.M. Seo, MepR, a repressor of the Staphylococcus aureus MATE family multidrug efflux pump MepA, is a substrate-responsive regulatory protein, Antimicrob. Agents Chemother. 50 (2006) 1276–1281.
[20] G.W. Kaatz, F. McAleese, S.M. Seo, Multidrug resistance in *Staphylococcus aureus* due to overexpression of a novel multidrug and toxin extrusion (MATE) transport protein, Antimicrob. Agents Chemother. 49 (2005) 1857–1864.
[21] B.D. Schindler, S.M. Seo, P.L. Jacinto, M. Kumaraswami, I. Birukou, R.G. Brennan, G.W. Kaatz, Functional consequences of substitution mutations in MepR, a repressor of the *Staphylococcus aureus* MepA multidrug efflux pump gene, J. Bacteriol. 195 (2013) 3651–3662.
[22] Z. Otwinowski, W. Minor, Processing of X-ray diffraction data collected in oscillation mode, Methods Enzym. 276 (1997) 307–326.
[23] A.J. McCoy, R.W. Grosse-Kunstleve, P.D. Adams, M.D. Winn, L.C. Storoni, R.J. Read, Phaser crystallographic software, J. Appl. Crystallogr. 40 (2007) 658–674.
[24] P. Emsley, K. Cowtan, Coot: model-building tools for molecular graphics, Acta Crystallogr. D Biol. Crystallogr. 60 (2004) 2126–2132.
[25] G.N. Murshudov, A.A. Vagin, E.J. Dodson, Refinement of macromolecular structures by the maximum-likelihood method, Acta Crystallogr. D Biol. Crystallogr. 53 (1997) 240–255.
[26] J. Liang, H. Edelsbrunner, P. Fu, P.V. Sudhakar, S. Subramaniam, Analytical shape computation of macromolecules: II. Inaccessible cavities in proteins, Proteins 33 (1998) 18–29.
[27] K.J. Newberry, M. Fuangthong, W. Panmanee, S. Mongkolsuk, R.G. Brennan, Structural mechanism of organic hydroperoxide induction of the transcription regulator OhrR, Mol. Cell 28 (2007) 652–664.
[28] V.B. Chen, W.B. Arendall 3rd, J.J. Headd, D.A. Keedy, R.M. Immormino, G.J. Kapral, L.W. Murray, J.S. Richardson, D.C. Richardson, MolProbity: all-atom structure validation for macromolecular crystallography, Acta Crystallogr. D Biol. Crystallogr. 66 (2010) 12–21.